**References and Notes**

(1) P. Haberfield, *J. Am. Chem. Soc.*, **96**, 6526 (1974).
(2) P. Haberfield, M. S. Lux, and D. Rosen, *J. Am. Chem. Soc.*, **99**, 6828 (1977).
(3) P. Haberfield, M. S. Lux, I. Jasser, and D. Rosen, *J. Am. Chem. Soc.*, **101**, 645 (1979).
(4) H. Baba, *Bull. Chem. Soc. Jpn.*, **34**, 76 (1961); H. Baba and S. Suzuki, *ibid.*, **34**, 82 (1961).
(5) H. Suzuki, "Electronic Absorption Spectra and Geometry of Organic Molecules", Academic Press, New York, 1965, p 478.
(6) (a) T. Förster, *Z. Elektrochem.*, **54**, 42 (1950); (b) E. L. Wehry and L. B. Rogers in "Fluorescence and Phosphorescence Analysis", D. M. Hercules, Ed., Interscience, New York, 1966, p 125, and references cited therein.
(7) P.-S. Song, *Photochem. Photobiol.*, **18**, 531 (1973); P.-S. Song and H. Baba, *ibid.*, **20**, 527 (1974).
(8) B. D. Pearson, *Proc. Chem. Soc., London*, 78 (1962); J. H. P. Utley, *J. Chem. Soc.*, 3252 (1963).
(9) Reference 5, p 493.
(10) M. J. Kamlet and R. W. Taft, *J. Am. Chem. Soc.*, **98**, 377 (1976); R. W. Taft and M. J. Kamlet, *ibid.*, **98**, 2886 (1976).
(11) The difference between the two net interaction energies ($\Delta H^{\text{solute-solvent}}$) is equal to the enthalpy of solvent transfer ($\delta\Delta H_{\text{DMF}\rightarrow\text{MeOH}}$) less the difference between the two solvent cavity formation energies ($\Delta H_{\text{solvent-solvent}}$) or $\delta\Delta H_{\text{DMF}\rightarrow\text{MeOH}} = \Delta H_{\text{solute-MeOH}} - \Delta H_{\text{solute-DMF}} + \Delta H_{\text{MeOH-MeOH}} - \Delta H_{\text{DMF-DMF}}$.
(12) R. Fuchs and R. F. Rodewald, *J. Am. Chem. Soc.*, **95**, 5897 (1973).
(13) P. P. Saluja, T. M. Young, R. F. Rodewald, F. H. Fuchs, D. Kohli, and R. Fuchs, *J. Am. Chem. Soc.*, **99**, 2949 (1977).
(14) E.g., M. J. Kamlet, E. G. Kayser, J. W. Eastes, and W. H. Gilligan, *J. Am. Chem. Soc.*, **95**, 5210 (1973).
(15) T. Yokoyama, R. W. Taft, and M. J. Kamlet, *J. Am. Chem. Soc.*, **98**, 3233 (1976).

# The Effect of Temperature on the Structure of Gaseous Molecules. 4. Molecular Structure and Barrier to Internal Rotation for Diboron Tetrabromide

**Donald D. Danielson and Kenneth Hedberg***

*Contribution from the Department of Chemistry, Oregon State University, Corvallis, Oregon 97331.* *Received November 2, 1978*

**Abstract:** The molecular structure of $B_2Br_4$ has been investigated by electron diffraction at nozzle temperatures of 23, 90, 150, and 305 °C. The molecule has a staggered equilibrium conformation (symmetry $D_{2d}$), with the following distances ($r_a$), angles, and root mean square amplitudes of vibration at room temperature: $r$(B–B) = 1.689 (16) Å, $r$(B–Br) = 1.902 (4) Å, ∠BrBBr = 120.7 (3)°, ∠BBBr = 119.8 (2)°, $l$(B–B) = 0.0552 Å (calculated from force field), $l$(B–Br) = 0.0526 (61) Å, $l$(B···Br) = 0.0948 (110) Å, $l$(Br···Br in $BBr_2$) = 0.0744 (36) Å; the parenthesized uncertainties are estimated 2$\sigma$. The average rotational barrier for the four temperatures based on a hindering potential assumed to have the form $2V = V_0(1 - \cos 2\phi)$ was found to be $V_0 = 3.07$ ($2\sigma = 0.33$) kcal/mol, higher than in either $B_2Cl_4$ (staggered) or $B_2F_4$ (planar). The estimated value of the torsional frequency is 18 cm$^{-1}$. The structure is discussed in comparison with those of $B_2F_4$ and $B_2Cl_4$, and a prediction for $B_2I_4$ is made.

## Introduction

Previous gaseous electron-diffraction investigations in this laboratory on $B_2F_4$[1] and $B_2Cl_4$[2] have yielded values both for the structural parameters of the molecules and for the barriers hindering internal rotation. $B_2F_4$ was found to be a slightly hindered rotor with a potential barrier of about 0.42 kcal/mol and to have a potential minimum when the $BX_2$ groups are eclipsed (symmetry $D_{2h}$). $B_2Cl_4$, however, was found to have a potential minimum in the staggered conformation (symmetry $D_{2d}$) and a considerably higher barrier of about 1.85 kcal/mol.

Our continuing interest in the diboron tetrahalides has led us to a similar investigation of $B_2Br_4$. The molecule was known to be structurally similar to the others, i.e., two $BX_2$ groups joined by a B–B bond. Moreover, interpretations of spectroscopic data[3] strongly suggested the equilibrium conformation to be staggered ($D_{2d}$ symmetry) in all three phases and thus to have a higher barrier to internal rotation than either $B_2Cl_4$ (staggered in the gas[2,4,5] and liquid,[4-6] eclipsed in the solid[4,7]) or $B_2F_4$ (eclipsed in all three phases[1,8,9]). Our particular interest was in the magnitude of the barrier, which we felt could be measured to good accuracy by electron diffraction, and in the geometrical details of the structure for comparison with $B_2Cl_4$ and $B_2F_4$. The description of our results follows.

## Experimental Section

Samples of $B_2Br_4$ were prepared and purified for us by Dr. David Kohler and Professor David Ritter of the University of Washington using known procedures.[10] Decomposition of $B_2Br_4$ into $BBr_3$ and a blackish solid of unknown composition was observed by these investigators to occur at a rate of about 28% per h at 38 °C in the gas phase at 5 Torr. To minimize this decomposition our samples were stored in liquid nitrogen baths between experiments.

In some early diffraction experiments the ground glass joints between the sample bulbs (equipped with Teflon vacuum stopcocks) and the injection nozzle were sealed with a silicone-base grease. This proved unacceptable owing to reaction at the seal producing, apparently, $SiBr_4$ as a contaminant. The grease was replaced with a single wrap of 0.08-mm thick Teflon tape and the joint externally packed with Dux-Seal. For one set of experiments at high temperature (305 °C) the glass joint was replaced with a Monel Swagelok fitting having a Nylon front ferrule and used in conjunction with a newly designed nozzle.[11] During all diffraction experiments the sample bulbs were maintained at temperatures between 7.0 and 11.5 °C. A slow discoloration suggestive of some decomposition was noted, but no evidence of impurity was found in the diffraction data.

Diffraction photographs were made in the Oregon State apparatus with an $r^3$ sector at four different nozzle-tip temperatures (23, 90, 150, and 305 °C) using 8 × 10 in. Kodak projector slide plates (medium contrast) developed for 10 min in D-19 developer diluted 1:1. Exposures were made for 30–210 s with pressures in the apparatus of 1.3 × $10^{-6}$ to 1.7 × $10^{-6}$ Torr at nozzle-to-plate distances of 75.017–75.161 (long camera) and 30.011–30.151 cm (middle camera). Undiffracted beam currents were 0.31–0.44 $\mu$A with wavelengths of 0.056 58–0.057 26 Å calibrated in separate experiments from diffraction patterns of $CO_2$ ($r_a$(CO) = 1.1646 Å, $r_a$(O···O) = 2.3244 Å). Remarkably, as in $B_2F_4$[1] and $BeB_2H_8$,[12] many of the plates were ruined by stains and streaks if developed immediately after exposure. As before, the problem was avoided by allowing the undeveloped plates

0002-7863/79/1501-3199$01.00/0 

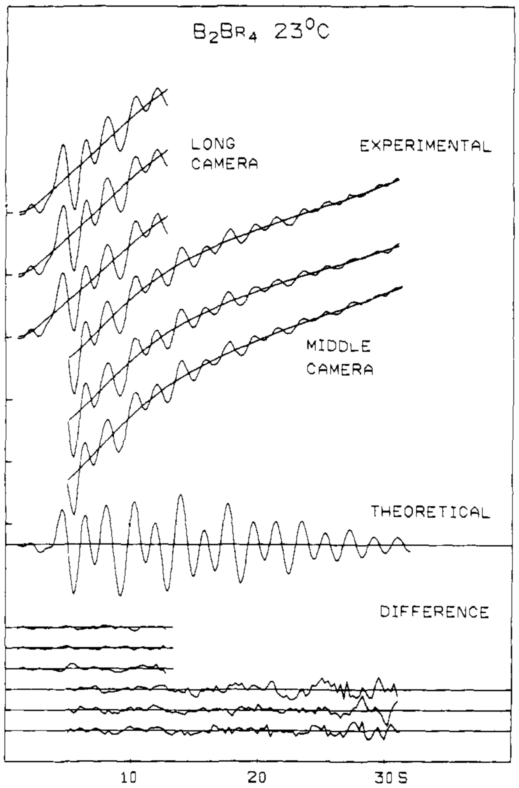


Figure 1. Intensity curves from experiments at 23 °C. The experimental curves are $s^4I_T$ shown superposed on the final backgrounds. The theoretical intensity curve is $sI_m$ for the model in Table III. The difference curves are the experimental minus the theoretical.

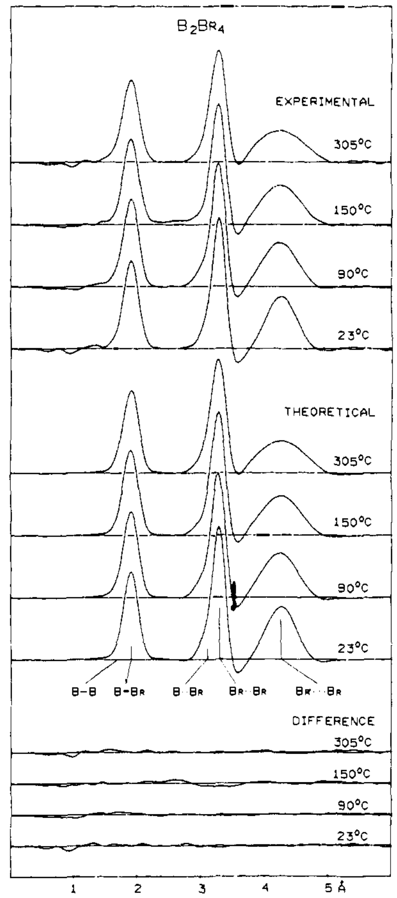


Figure 2. Radial distribution curves. The experimental curves are calculated from composites of molecular intensities exemplified in Figure 1. The theoretical curves correspond to the models in Table III. The difference curves are experimental minus theoretical.

to stand in contact with the atmosphere for about 24 h followed by rinsing in water immediately before development. Three plates from each camera distance at each temperature (24 in all) were used in the structure analysis.

## Reduction of Data and Radial Distribution Curves

Procedures for obtaining the scattered intensity distribution $s^4I_T$ have been described.[13] Backgrounds were calculated[14] and subtracted from the data from each plate to give intensity data in the form represented by

$$sI_m(s) = k \sum_{i \neq j} A_iA_jr_{ij}^{-1} \cos|\eta_i - \eta_j| V_{ij} \sin s(r_{ij} - \kappa_{ij}s^2) \tag{1}$$

The range of the data was $2.00 \leq s \leq 31.75$ Å for each temperature. Curves of the total scattered intensities, the final backgrounds, and the theoretical molecular intensities are shown in Figure 1 for the 23 °C experiments. The corresponding figures for the other three temperatures and all the data for these curves are available as supplementary material.

Radial distribution curves were calculated from composite intensity curves according to

$$rD(r) = \frac{2}{\pi} \Delta s \sum_{s=0}^{s_{max}} I'(s) \exp(-Bs^2) \sin rs \tag{2}$$

in which $I'(s) = sI_m(s)Z_BZ_{Br}A_B^{-1}A_{Br}^{-1}$ and $B = 0.0025$ Å$^2$. The modified scattering amplitudes $A_i$ were obtained[13] from tables.[15] For the experimental radial distribution curves, data for the unobserved or uncertain region $s < 2.00$ Å$^{-1}$ were taken from theoretical intensity curves.

The final radial distribution curves are shown in Figure 2. The presence of only a single peak at about 4.3 Å corresponding to the torsion-sensitive Br···Br distance reveals immediately that the molecule has a staggered conformation: an eclipsed conformation would be reflected in two peaks at about 3.6 and 4.9 Å arising from cis and trans Br···Br distances.

## Structure Analysis

Structure refinements were carried out by least squares based on intensity curves[16] in the form of eq 1 by simultaneously adjusting a single theoretical curve to the six sets of data from each temperature. A unit weight matrix and the harmonic-vibration approximation with $\kappa = 0$ and $V_{ij} = \exp(l_{ij}^2s^2/2)$ were assumed. The geometrical parameters were taken to be the two bond distances and the Br–B–Br bond angle. The vibrational amplitude parameters ($l$'s) were three of the four for the torsion-insensitive distances; $l_{B-B}$ could not be independently refined and was given values calculated from an approximate force field.

The potential barrier was also treated as a parameter by taking account of its effect on the torsion-sensitive distance distribution through the least-squares procedure. We adopted the low-barrier classical approximation for the probability distribution of rotational angle

$$P(\phi) = [\exp(-V(\phi)/RT]/Q \tag{3}$$

and assumed the potential function to be $2V(\phi) = V_0(1 - \cos 2\phi)$ with $\phi = 0$ in the staggered conformation. The continuous torsion-sensitive distance distribution was approximated by calculating distances $r_{Br\cdots Br}(\phi)$ at angle increments $\Delta\phi = 10°$ over the range $0° \leq \phi \leq 90°$, weighting each according to $P(\phi)$, and assigning each an amplitude of vibration calculated without cognizance of torsional motion ("frame" amplitude). The number of distinct distances generated by this scheme included the four torsion-independent ones and 19 weighted,

**Table I.** Structural Results for $BrBr_4$[a]

| | 23 °C | | 90 °C | | 150 °C | | 305 °C | |
|---|---|---|---|---|---|---|---|---|
| | $r_a$ | $l$ | $r_a$ | $l$ | $r_a$ | $l$ | $r_a$ | $l$ |
| B-B | 1.689 (16) | 0.0552[b] | 1.665 (16) | 0.0558[b] | 1.688 (20) | 0.0566[b] | 1.702 (33) | 0.0595[b] |
| B-Br | 1.902 (4) | 0.0526 (61) | 1.899 (3) | 0.0589 (58) | 1.900 (3) | 0.0616 (56) | 1.902 (5) | 0.0676 (75) |
| B···Br | 3.098 (12) | 0.948 (110) | 3.072 (14) | 0.1123 (110) | 3.090 (18) | 0.1369 (144) | 3.098 (29) | 0.1469 (259) |
| Br···Br | 3.293 (4) | 0.744 (36) | 3.284 (4) | 0.0828 (39) | 3.282 (4) | 0.0379 (41) | 3.279 (6) | 0.1024 (57) |
| Br···Br ($\phi$ = 0) | 4.247 (22) | 0.1563[c] | 4.217 (22) | 0.1730[c] | 4.235 (25) | 0.1866[c] | 4.236 (14) | 0.2178[c] |
| ∠BrBBr[d] | 120.7 (3) | | 120.7 (3) | | 120.6 (3) | | 120.8 (5) | |
| $V_0$ | 3.30 (85) | | 2.98 (63) | | 2.97 (54) | | 3.18 (73) | |
| $R$[e] | 0.153 | | 0.146 | | 0.139 | | 0.209 | |

[a] Distances and amplitudes in ångstroms, angles in degrees, and barriers in kcal/mol. [b] Calculated amplitude. [c] Calculated frame amplitude. [d] Angles are $\alpha$-space angles. [e] $R = [\Sigma\omega_i\Delta_i^2/\Sigma\omega_i(sI_i^{\text{obsd}}(s))^2]^{1/2}$ where $\Delta_i = sI_i^{\text{obsd}}(s) - sI_i^{\text{calcd}}(s)$.

**Table II.** Correlation Matrix for Final Model at 23 °C (×10$^2$)[a]

| | $r_{B-B}$ | $r_{B-Br}$ | ∠BrBBr | $l_{B-Br}$ | $l_{B\cdots Br}$ | $l_{Br\cdots Br}$ | $V_0$ |
|---|---|---|---|---|---|---|---|
| $\sigma_{LS}$[b] | 0.55 | 0.11 | 12.2 | 0.20 | 0.37 | 0.07 | 14.5 |
| | 100 | −41 | 53 | −42 | −11 | −37 | 22 |
| | | 100 | −94 | 4 | 4 | 5 | 1 |
| | | | 100 | −8 | −12 | −10 | 1 |
| | | | | 100 | 3 | 45 | 25 |
| | | | | | 100 | 34 | −2 |
| | | | | | | 100 | −28 |
| | | | | | | | 100 |

[a] Distances and amplitudes in ångstroms, angles in degrees, and barriers in kcal/mol. [b] From least-squares refinement.

torsion-sensitive ones arising from the chosen angle interval. The $r_a$ values of these distances used in eq 1 were generated from the geometrically consistent $r_\alpha$ set according to

$$\begin{aligned} r_a &= r_\alpha + K - l^2/r_a \\ &= r_g - l^2/r_a \end{aligned} \qquad (4)$$

using experimental $l$ values in the cases of the three refinable amplitudes and calculated values for $l_{B-B}$, for the frame $l$ corresponding to the 19 torsion-sensitive distances, and for the perpendicular amplitudes $K$, all obtained as described in the next section. Because the values of $K$ for the torsion-independent distances differed slightly for the different fixed conformations, the values calculated for $\phi$ = 20°, which were good approximations (to within 2%) to the weighted averages, were adopted.

Since $B_2Br_4$ is known to decompose into $BBr_3$ (and heavier, less volatile products), tests for the possible presence of $BBr_3$ in the sample were felt to be necessary. This was done by introducing it as a second component of known structure[17] and refining the composition of the mixture as a parameter. The results showed no detectable $BBr_3$ at any of the experimental temperatures[18] and accordingly contamination of the gas samples by this material was assumed to be negligible and ignored in the remaining work.

## Normal Coordinate Calculations

The perpendicular amplitudes and the amplitudes of vibration which could not be obtained from the diffraction experiment and which were needed in our model of $B_2Br_4$ were calculated from an approximate force field adjusted to fit the observed wavenumbers.[3] These calculated quantities were needed at each of the four temperatures for each of the ten torsionally rigid, hypothetical conformers used to generate the approximation to the torsion-sensitive distance distribution. They were obtained by interpolation from smooth curves drawn through values calculated for just five rotamers ($\phi$ = 0, 20, 45, 70, and 90°). The calculations assumed the same force field for each conformer. Complete tabulations of the calculated frame amplitudes, perpendicular amplitudes, symmetry coordinates, and symmetrized force constants are available as supplementary material.

## Results and Discussion

**Structure and Conformation.** The results of the final least-squares refinements are given in Table I and the correlation matrix for the 23 °C experiment in Table II; the other correlation matrices appear in the supplementary material. The interatomic distances (with due regard for the listed uncertainties) are consistent at all temperatures, but it must be admitted that the values for the 90 °C case generally tend to be slightly smaller than those for the corresponding distances at the other temperatures. If these differences indeed reflect an error in the size of the molecule caused, say, by an error in wavelength or camera-length measurement, one expects the error to have no effect on the angle and amplitude parameters or on the value of the barrier $V_0$. This is seen to be so. We note also in passing that, despite the agreement of the parameter values at the highest temperature with those at the lower, the quality of the fit as measured by the value of $R$ is distinctly worse. This quantitative evidence is qualitatively recognizable in one of the intensity-difference curves from the intermediate camera distance: this curve is rather more noisy than any other irrespective of temperature or camera distance.

The values for the B-Br bond length and terminal Br···Br distance in $B_2Br_4$ are little different from the corresponding ones in $BBr_3$ ($r_a$(B-Br) = 1.892 ± 0.005 Å, $r_a$(Br···Br) = 3.281 ± 0.005 Å, as calculated from eq 4 from the published $r_g$ values[18]). A similar situation is found for $B_2Cl_4$ and $BCl_3$, and for $B_2F_4$ and $BF_3$, and suggests that the bonding at the boron atom is nearly identical in the tri- and tetrahalides.

Table III summarizes structural details of the molecules $B_2F_4$, $B_2Cl_4$, and $B_2Br_4$. We have discussed[1,2] structures of the tetrafluoride and tetrachloride in terms of effects implied by structures such as I and II competing with steric repulsions arising between vicinally situated bonds or halogen atoms. Those arguments may be extended to include $B_2Br_4$. They are, essentially, that the conjugation implied by the above diagrams favors molecular planarity whereas the steric effects favor a

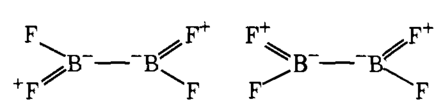

I II

**Table III.** Structural Parameter Values for $B_2F_4$, $B_2Cl_4$, and $B_2Br_4$

| | $B_2F_4$ | $B_2Cl_4$ | $B_2Br_4$ |
|---|---|---|---|
| exptl temp, °C | +22 | −22 | +23 |
| molecular symmetry | $D_{2h}$ | $D_{2d}$ | $D_{2d}$ |
| distances, $r_a$, Å | | | |
| B–X | 1.317 (2) | 1.750 (11) | 1.902 (4) |
| B–B | 1.720 (4) | 1.702 (69) | 1.689 (16) |
| B···X | 2.656 (4) | 3.000 (49) | 3.098 (12) |
| X··X | 2.247 (3) | 3.011 (8) | 3.293 (4) |
| X···X | 3.093 (10); 3.823 (10) | 4.087 (40) | 4.247 (22) |
| angles, deg | | | |
| XBX | 117.2 (2) | 118.7 (7) | 120.7 (3) |
| XBB | 121.4 (1) | 120.6 (4) | 119.7 (2) |
| rotational barrier, kcal mol$^{-1}$ | 0.42 (16) | 1.85 (5) | 3.07 (33) |
| ref | 1 | 2 | this work |

staggered conformation. Specifically, familiar arguments predict I and II to be most important for the fluoride and least so for the bromide. On the other hand, repulsive forces in planar forms of the molecules are estimated to be least for the fluoride and greatest for the bromide based on the differences between hypothetical or actual cis X···X distances and the sum of the van der Waals radii: cis minus vdW equals +0.39 Å for $B_2F_4$, −0.11 Å for $B_2Cl_4$, and −0.33 Å for $B_2Br_4$. In a qualitative sense one may view the result of the two effects as a near-balancing in the case of planar $B_2F_4$ where the barrier to rotation is relatively small, a significant domination of repulsion in staggered $B_2Cl_4$ with its greater barrier, and a very pronounced domination of repulsion in staggered $B_2Br_4$ with its still greater barrier.

The above considerations may also be invoked to account for the B–X and B–B bond lengths. The B–X distances are observed to be substantially less (0.05–0.06 Å) in $B_2F_4$ and slightly greater (0.01–0.03 Å) in $B_2Cl_4$ and $B_2Br_4$ than the covalent radius sum corrected for electronegativity difference;[19] these differences agree qualitatively with the greater importance of structures I and II in the case of the fluoride. The B–B distances (Table III) are interesting because they differ in a way contrary to expectation based on conjugation effects which, other things being equal, should shorten this distance in the fluoride relative to those in the other molecules. Assuming that the observed trend $B\text{–}B_F > B\text{–}B_{Cl} > B\text{–}B_{Br}$ is indeed real (the large uncertainties engender some skepticism), the trend may be attributed to an effect which overwhelms the effect of conjugation, namely, Coulomb repulsions between the boron atoms which bear residual charges arising from the ionic character of the B–X bonds. We note first that conjugation shortening of the B–B bonds cannot be expected to exceed a few thousandths of an ångstrom even in $B_2F_4$. The reason is that in reasonable model compounds such as oxalyl chloride[20] and glyoxal,[21] with essentially pure carbonyl double bonds in contrast to the 18–21% partial double bond character estimated[22a] for the B–F links in $B_2F_4$, the conjugation shortening of the central bonds is only about 0.015 Å. On the other hand, the ionic character of the B–F, B–Cl, and B–Br bonds is estimated[22b] to be 63, 22, and 15%, respectively, and, although some back transfer of the charges implied by these numbers through double bond formation is likely, the remaining charges would seem to be more than sufficient to counteract the weak effects of conjugation. All in all the observed variations in the B–B bond lengths among the three tetrahalides cannot be regarded as unusual.

**Vibrational Amplitudes, Shrinkages, and Force Field.** The observed and calculated amplitudes (Tables I and IV) for $l_{B-Br}$ and $l_{Br\cdots Br}$ are generally in very good agreement at all temperatures, but the observed value for $l_{B\cdots Br}$ appears to be uniformly larger than the calculated one by almost exactly the uncertainties in the measurements. This systematic effect is puzzling but hardly worrisome, and in any event can have no effect on the molecular properties of most interest. The shrinkages (Table V) have appreciable magnitudes, and, because they involve distances of high weight, play an important role in the quality of fit to the data. The agreement between calculated and observed intensities was found to be much worse when the shrinkages were ignored.

The nonunique quadratic force field from which our calculated $l$'s and $K$'s were derived has no special virtue, but it appears to be as reasonable as any other giving a fit to the fundamental vibrational wavenumbers. It was obtained by the symmetrization of a set of bond-stretching, angle-bending, and out-of-plane-bending constants taken from similar molecules and adjusting the symmetrized set to minimize as much as possible the values of certain off-diagonal constants. The values used are not much different from the original set and thus may be assumed to be consistent with stretching and bending constants for similar bonds and bond angles. A matter for concern

**Table IV.** $B_2Br_4$. Calculated Amplitudes and $r_a$ Shrinkages[a,b]

| | 23 °C | | | 90 °C | | | 150 °C | | | 305 °C | | |
|---|---|---|---|---|---|---|---|---|---|---|---|---|
| | $l$ | $K$ | shkg[c] | $l$ | $K$ | shkg[c] | $l$ | $K$ | shkg[c] | $l$ | $K$ | shkg[c] |
| B–B | 0.0551 | 0.0055 | | 0.0558 | 0.0063 | | 0.0566 | 0.0070 | | 0.0595 | 0.0090 | |
| B–Br | 0.0527 | 0.0111 | | 0.0546 | 0.0134 | | 0.0565 | 0.0154 | | 0.0618 | 0.0021 | |
| B··Br | 0.0848 | 0.0057 | 0.008 | 0.0915 | 0.0069 | 0.009 | 0.0972 | 0.0080 | 0.014 | 0.1111 | 0.0107 | 0.018 |
| Br··Br | 0.0739 | 0.0044 | 0.013 | 0.0812 | 0.0054 | 0.017 | 0.0871 | 0.0063 | 0.019 | 0.1011 | 0.0087 | 0.029 |
| Br···Br[d] | 0.1563 | 0.0014 | 0.021 | 0.1730 | 0.0017 | 0.026 | 0.1866 | 0.0020 | 0.031 | 0.2178 | 0.0027 | 0.041 |

[a] Values in ångstroms. [b] Amplitudes ($l$) and perpendicular amplitudes ($K$) from force field. See supplementary material. [c] The difference between distances calculated from the $r_a$ bond lengths and bond angles of Table I and the measured values. [d] Frame amplitudes for rotamer with ∠$Br_2B$, $BBr_2$ equal to 90°.

**Table V.** Uncertainties in $V_0$ Estimated from Least-Squares Fit and Dependence of $V_0$ on $l_{Br\cdots Br}$[a]

| 23 °C | | | 90 °C | | | 150 °C | | | 305 °C | | |
|---|---|---|---|---|---|---|---|---|---|---|---|
| $l$ | $V_0$ | $\sigma_F$[b] | $l$ | $V_0$ | $\sigma_F$[b] | $l$ | $V_0$ | $\sigma_F$[b] | $l$ | $V_0$ | $\sigma_F$[b] |
| 0.1263 | 2.806 | 0.142 | 0.1430 | 2.650 | 0.137 | 0.1566 | 2.722 | 0.142 | 0.1878 | 3.036 | 0.262 |
| 0.1563[c] | 3.302 | 0.206 | 0.1730[c] | 2.984 | 0.184 | 0.1866[c] | 2.970 | 0.185 | 0.2178[c] | 3.185 | 0.333 |
| 0.1863 | 4.243 | 0.358 | 0.2030 | 3.527 | 0.275 | 0.2166 | 3.358 | 0.258 | 0.2478 | 3.436 | 0.432 |
| $\delta_l$[d] | 0.374 | | | 0.253 | | | 0.198 | | | 0.145 | |
| $2\sigma_v$[e] | 0.85 | | | 0.63 | | | 0.54 | | | 0.73 | |

[a] $l$ in angstroms; $V_0$, $\sigma$, and $\delta$ in kcal/mol. [b] Uncertainty in $V_0$ from least-squares refinements. [c] Frame values calculated from force field. [d] Average value of the change in $V_0$ for 10% change in $l_{Br\cdots Br}$. [e] Estimated uncertainty in $V_0$ calculated according to $2\sigma_v = 2(\sigma_F^2 + \delta_l^2)^{1/2}$.

is the possible sensitivity of the calculated $l$'s and $K$'s to the force field. The conventional view is that they are not very sensitive, a view we have verified in tests of several cases including $B_2Br_4$. We conclude that the experimental results we are reporting would not be changed significantly with any plausible change in the force field.

**Rotational Barrier, Torsional Amplitude, and Torsional Frequency.** Our method for determining $V_0$ as a part of our least-squares procedure is based upon a separation of internal rotation from other vibrational modes and requires that one estimate the effect of these other modes on the torsional-sensitive distances. This was done by calculation of the frame amplitudes of vibration as described in an earlier section, and raises the question of the effect of error in these frame amplitudes on the value deduced for the barrier. We tested the matter by carrying out refinements of $V_0$ with the frame amplitudes for the torsion-sensitive distances arbitrarily increased and decreased by 10% from the calculated values; these changes represent a reasonable guess of possible error based on experience. The values of $V_0$ are given in Table V with uncertainties that include the uncertainty in fit ($\sigma_F$) and the uncertainty in the frame amplitudes ($\delta_l$) calculated according to $2\sigma = 2(\sigma_F{}^2 + \delta_l{}^2)^{1/2}$. The individual values are pleasingly consistent and correspond to an average (weighted inversely as the square of the uncertainties) of 3.07 ($2\sigma = 0.33$) kcal mol$^{-1}$. The barrier is thus considerably larger than in $B_2Cl_4$ ($1.85 \pm 0.07$ kcal mol$^{-1}$) and in $B_2F_4$ ($0.42 \pm 0.16$ kcal mol$^{-1}$).

The radial distribution curves offer striking evidence for the effect of temperature on the torsional amplitude: the peak at 4.2 Å arising from the torsion-sensitive Br···Br distance has, at the lowest temperature, distinctly Gaussian character which changes to a much broader, rounded form at the highest. This change is completely consistent with our assumed form for the rotational potential, $2V = V_0(1 - \cos 2\phi)$. With a high barrier as in $B_2Br_4$ the torsional amplitude is relatively small at low temperatures and the potential is approximately described by only the quadratic term $V_0\phi^2$ in the series expansion; eq 3 then predicts an essentially Gaussian distribution of torsional angle and torsion-sensitive distances. At high temperatures other terms in the expanded form of the potential play an important role. The root mean square torsional amplitude calculated from eq 3 using the $V_0$'s of Table IV have values of 19.2, 19.9, 24.5, 27.1, and 31.2°; the value at the lowest temperature using the harmonic approximation is 17.8°.

An estimate of the torsional wavenumber may be made from the formula $\omega = (2\pi c)^{-1} (k_\phi/\mu_1)^{1/2}$ where $k_\phi = 2V_0$ and $\mu_1$ is the reduced moment of inertia of the $BBr_2$ groups around the B–B bond. The result is 18 cm$^{-1}$ ($2\sigma = 4$ cm$^{-1}$), too low to have been seen in measurements of the Raman spectrum[3] down to 30 cm$^{-1}$.

**Predictions about $B_2I_4$.** A possible preparation of $B_2I_4$ has recently been reported.[23] The structural work on the three lower diboron tetrahalides provides a clear picture of trends in the bond distances and bond angles and allows one to predict the properties of the very unstable iodine compound with considerable confidence. Thus, the molecular symmetry is expected to be $D_{2d}$ as in the chloride and bromide, and the barrier to internal rotation about 4.4 kcal mol$^{-1}$. The B–B bond length should be about 1.69 Å and the B–I about 2.10 Å. We believe that the I–B–I bond angle will be slightly larger than in the chloride and bromide: at 123° this angle together with the predicted B–I bond length corresponds to geminal I···I distance which is less than the sum of the van der Waals radii by the same amount as is found for the chloride and bromide.

**Acknowledgment.** We are grateful to Professor David Ritter and to Dr. David Kohler for the samples of $B_2Br_4$, to Dr. Lise Hedberg for much helpful discussion, and to the National Science Foundation, which supported this work under Grants CHE74-13527 and CHE78-04258.

**Supplementary Material Available:** Tables of total intensities and final backgrounds at all temperatures, of correlation matrices at 90, 150, and 305 °C, and of frame amplitudes, perpendicular amplitudes, symmetry coordinates, and symmetrized force constants; curves of intensity data at 90, 150, and 305 °C; diagram of molecule and internal coordinates (37 pages). Ordering information is given on any current masthead page.

## References and Notes


(1) D. D. Danielson, J. V. Patton, and K. Hedberg, *J. Am. Chem. Soc.*, **99**, 6484 (1977).
(2) R. R. Ryan and K. Hedberg, *J. Chem. Phys.*, **50**, 4986 (1969).
(3) J. D. Odom, J. E. Saunders, and J. R. Durig, *J. Chem. Phys.*, **56**, 1643 (1972).
(4) J. R. Durig, J. E. Saunders, and J. D. Odom, *J. Chem. Phys.*, **54**, 5285 (1971).
(5) D. E. Mann and L. Fano, *J. Chem. Phys.*, **26**, 1665 (1957).
(6) L. A. Nimon, K. S. Seshadri, R. C. Taylor, and D. White, *J. Chem. Phys.*, **53**, 2416 (1970).
(7) M. Atoji, P. J. Wheatley, and W. N. Lipscomb, *J. Chem. Phys.*, **27**, 196 (1957).
(8) J. R. Durig, J. W. Thompson, J. D. Witt, and J. D. Odom, *J. Chem. Phys.*, **58**, 5339 (1973).
(9) L. Trefanus and W. N. Lipscomb, *J. Chem. Phys.*, **28**, 54 (1958).
(10) G. Urry, T. Wartik, R. E. Moore, and H. I. Schlesinger, *J. Am. Chem. Soc.*, **76**, 5293 (1954).
(11) A description will be published elsewhere.
(12) G. Gundersen, L. Hedberg, and K. Hedberg, *J. Chem. Phys.*, **59**, 3777 (1973).
(13) G. Gundersen and K. Hedberg, *J. Chem. Phys.*, **51**, 2500 (1969).
(14) L. Hedberg, Abstracts, Fifth Austin Symposium on Gas Phase Molecular Structure, Austin, Texas, March 1974, p 37.
(15) L. Schäfer, A. C. Yates, and R. A. Bonham, *J. Chem. Phys.*, **55**, 3055 (1971).
(16) K. Hedberg and M. Iwasaki, *Acta Crystallogr.*, **17**, 529 (1964).
(17) S. Konaka, T. Ito, and Y. Morino, *Bull. Chem. Soc. Jpn.*, **39**, 1146 (1966).
(18) Although at first sight surprising, this result is consistent with the low residence time of the gas in the nozzle (~0.1 s) and decomposition rate mentioned earlier in the text for 38 °C: a rough estimate based on a 1000-fold increase in rate over the range 38–305 °C is less than 1% decomposition.
(19) V. Schomaker and D. P. Stevenson, *J. Am. Chem. Soc.*, **63**, 37 (1941). The factor 0.08 is used in the electronegativity correction.
(20) K. Hagen and K. Hedberg, *J. Am. Chem. Soc.*, **95**, 1003 (1973).
(21) K. Kuchitsu, T. Fukuyama, and Y. Morino, *J. Mol. Struct.*, **1**, 463 (1967).
(22) (a) L. Pauling, "The Nature of the Chemical Bond", 3rd ed., Cornell University Press, Ithaca, N.Y., 1960, Chapter 7; (b) *ibid.*, Chapter 3.
(23) B. V. Zhuk, G. A. Dormacker, and A. M. Ob'edkov, *Izv. Akad. Nauk SSSR, Ser Khim.*, **5**, 1201 (1977).